Robustness of Features for Automatic Target Discrimination in High Resolution Polarimetric SAR Data

Albertus van den Broek, Rob Dekker, and Philippe Steeghs

TNO Physics and Electronics Laboratory, P.O. Box 96864, 2509 JG The Hague, The Netherlands

ABSTRACT

We have studied the robustness of features against aspect variability for the purpose of target discrimination using polarimetric 35 Ghz ISAR data. Images at a resolution of 10 cm and 30 cm have been used for a complete aspect range of 360 degrees. The data covered four military targets: T72, ZSU23/4, T62, and BMP2. For the study we composed several feature vectors out of individual features extracted from the images. The features are divided into three categories: radiometric, geometric and polarimetric. We found that individual features show a strong variability as a function of aspect angle and cannot be used to discriminate between the targets irrespectively of the aspect angle. Using feature vectors and a maximum likelihood classifier reasonable discrimination (about 80%) between the four targets irrespective of the aspect angle was obtained at 10 cm resolution. At 30 cm resolution less significant discrimination (less than 70%) was found irrespective of the kind of feature vector used. In addition we investigated target discrimination per 30-degree aspect interval. In order to determine the aspect angle of targets we used a technique based on the Radon transformation, which gave an accuracy of about 5 degrees in aspect angle. We found that in this case good discrimination (more than 90%) was obtained at 10 cm resolution and reasonable discrimination (about 80%) at 30 cm resolution. The results are compared with analogous results from MSTAR data (30 cm resolution) of comparable targets.

Keywords: SAR, aspect angle, Radon transformation, target discrimination, robust features

1. INTRODUCTION

With the increasing use of UAVs for RSTA purposes also the interest in SAR imaging systems is growing, because of their unparalleled all-time and all-weather capability. In this context a study for the Dutch MOD was defined in which the role of SAR for ground surveillance is investigated. This study is carried out within the framework of the NATO/SET/TG14 research group, which focuses on robust acquisition of relocatable targets with advanced millimetre wave techniques. By participating in the group we have access to a database with high resolution SAR and ISAR data for various targets and scenes. This database was created and is maintained by the group to study automatic target recognition techniques in the millimetre wave domain. The US Army Research Laboratory (ARL) has contributed to the database with high-resolution (10cm) polarimetric ISAR data of four military targets at 35 Ghz. These data comprised two main battle tanks (T72, T62) an air defence unit (ZSU-23-4) and an infantry-fighting vehicle (BMP2).

We have used these data for studying features, which are able to discriminate targets in high resolution SAR data. The study presented here focuses on the robustness of features against aspect angle variability. A second objective is to develop techniques for accurate determination of the aspect angle of targets. If the aspect angle can be measured with sufficient accuracy the robustness of features has to be valid only for smaller aspect intervals. We have used Radon transformation and feature-enhanced processing for this purpose. In order to compare the ISAR data with targets extracted from SAR measurements we have analysed MSTAR data of comparable targets in a similar way.

The paper is organised as follows. In section 2 we describe the data. In section 3 we introduce and describe the features used in the study. In section 4 we analyse the robustness of these features by combining them into feature vectors and by considering aspect angle intervals. Section 6 focuses on the aspect angle determination techniques, which include Radon transformation and feature-enhanced processing. Finally, in section 5 we give a summary.

---

2. DESCRIPTION OF THE DATA

2.1 High resolution polarimetric ISAR data

The ARL-ISAR measurements were performed with a fully polarimetric stepped frequency radar. The measured data are in the frequency domain and the spatial domain image is obtained through a 2-D inverse FFT (Chen and Andrews 1980). The range and azimuth (i.e. cross-range) resolution of the generated images are determined by

$$\delta_r = \frac{c}{2\Delta f}, \tag{1}$$

$$\delta_a = \frac{\lambda}{2\Delta \theta}. \tag{2}$$

Here, Δf is the bandwidth of the transmitted sweep, $\Delta \theta$ the angle of rotation or coherence interval, and λ the wavelength. Weighting was applied to reduce the sidelobes of the impulse response by applying the following window in the frequency domain

$$h(n) = \frac{1+w}{2} + \frac{1-w}{2} \cos\left(2\pi \frac{n-N/2}{N}\right). \tag{3}$$

Here w is the weighting factor and N the FFT length. We have chosen a weighting factor of 0.5, and consequently the decrease in resolution will be small. The following table summarizes the main properties of the data and images.

Table 1. ARL-ISAR data parameters

Band	Ka
Centre frequency	34.25 GHz
Bandwidth	1511.64 MHz
Frequency step	5.928 MHz
Nr. of samples (range)	256
Resolution (range)	10 cm
Coherence interval	2.4°
Angle sampling interval	0.015°
Nr. of samples (azimuth)	160
Resolution (azimuth)	10 cm
Polarisations	HH, HV, VH, VV
Depression angle	10° (BMP2, T72, T62) and 12° (ZSU23-4)
Incidence angle	80° (BMP2, T72, T62) and 78° (ZSU23-4)
Number of looks	Single Look

In this way a set of 794 fully polarimetric 10 cm resolution images was created covering the complete range of 360 degrees of aspect. This implies one image for every 0.45 degree of aspect. We also produced a similar second set of 30 cm resolution images by using a third of $\Delta\theta$ and Δf compared the 10 cm resolution images. This was done to be able to compare the results with those obtained for the MSTAR data. In Figure 1 we show 10 cm ARL-ISAR images for the T62, T72, BMP and ZSU targets for one aspect angle.
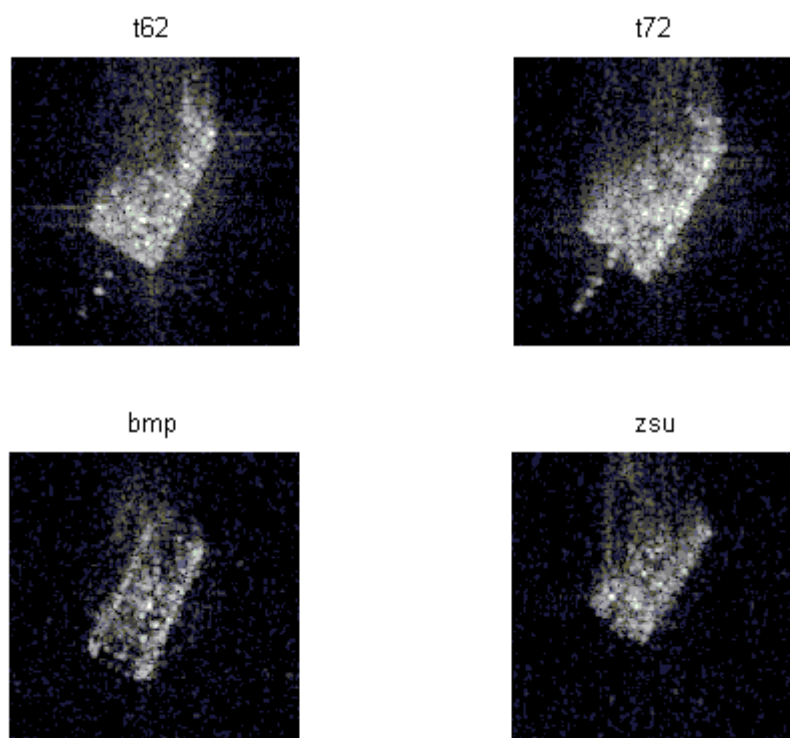
Figure 1. ARL-ISAR 10 cm resolution images for the T62, T72, BMP and ZSU targets.

2.2 MSTAR data

MSTAR data from the public database were used for comparison. These data were taken from data collection 1 (September 1995) and data collection 2 (November 1996). Data were collected at X-band, HH polarisation with about 30 by 30 cm resolution for various aspect angles covering the complete circle of 360 degrees. The depression angle of the selected data was 15 degrees. See Table 2 for further details.

Table 2. MSTAR data

Target	MSTAR data collection	Type
T62	data collection #2, scene 1	T62
T72	data collection #1	T72 variant SN_812
BMP	data collection #1	BMP-2 variant SN_9563
ZSU	data collection #2, scene 1	ZSU 23/4

We use the results from the MSTAR data for comparison with the results from the ARL-ISAR data. The comparison is not straightforward since there are differences in elevation angle (15 degrees versus 12/10 degrees) and the frequency band (Ka band versus X-band) used.

For the study we used three cases. For the first case we calculated fully polarimetric images for 794 aspect angles with a resolution of 10 cm from the ARL-ISAR data. For the second case we calculated fully polarimetric images for the same 794 aspect angles with a resolution of 30cm, which can be used for comparison with the MSTAR data (third case). The MSTAR data comprised 275, 195, 196 and 276 aspect angles for the T62, T72, BMP and ZSU targets respectively.

3. FEATURE EXTRACTION

3.1. Description of method

We selected three classes of features: radiometric, geometric and polarimetric. For each class three features were identified, which are expected to give independent information and are characteristic for the class they belong. Table 3 summarises the features used.

Table 3. Categories of features used

Radiometric		Geometric		Polarimetric	
MEAN	mean intensity	*AREA*	area of target	*HHHV*	polarimetric (HH/HV) power ratio
CVAR	coefficient of variation	*NN*	neighbour number	*EVEN*	percent odd
WFR	Weighted rank fill ratio	*LAC*	lacunarity index	*ODD*	percent even

As a basis to calculate the feature values we first used a CFAR detector (Novak and Hesse 1991) to detect target pixels. The CFAR constant was chosen using the average background in the image and such that on average about 30% of the pixels that cover the geometric extent of the target were detected. For the MSTAR data this means a constant of about -5 dB. In this way almost no background pixels were detected. The same criterion with a comparable constant was applied to HH-polarised images calculated from the ARL-ISAR data. Note that for the ARL-ISAR images there is no background present. Figure 3 shows an example of the detected target pixels compared with the original image. Computation of all feature values is done using only the detected target pixels. Below we give a short description of the features.
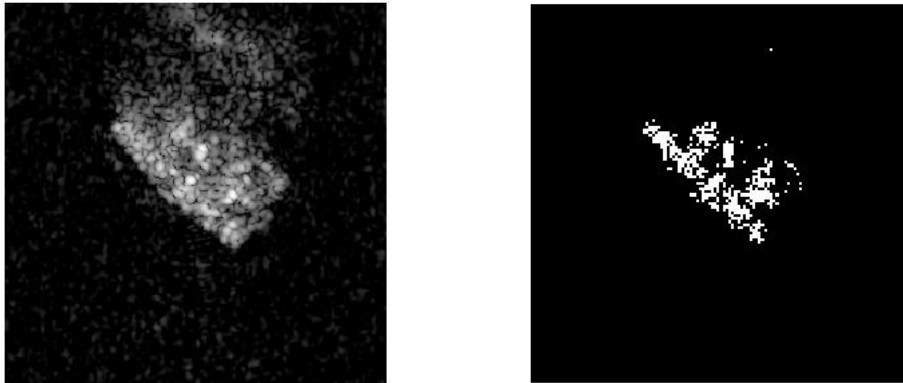
Figure 3. 10 cm ARL-ISAR image and the detected CFAR pixels for the ZSU target.

MEAN: The mean (μ) of the power of the detected target pixels, which indicates how bright the target appears in the image.

CVAR: The normalized variance of the power of the detected target pixels defined by

$$cv = \frac{\sigma^2}{\mu^2}.$$

(4)

This feature indicates how smooth or not the scattering is distributed over the target.

WFR: This measure is defined as the ratio of the sum of the power of the *N* brightest pixels, and the sum of power of all detected pixels (Kreithen et al. 1993). For the 10 cm resolution images we took N=75 and for the 30 resolution images we took N=10. This feature measures the relative amount of scattering due to 'hot spots'.

AREA: The number of detected target pixels. This feature clearly indicates the geometric extent of the target.

NN: The neighbour number is a measure for the spatial distribution of the CFAR detected target pixels (van den Broek et al., 2001). The number is defined by total number of neighbour pixels of all detected pixels normalized by the total number of detected pixels. This feature is a kind of texture measure indicating how well detected pixels are lumped together.

LAC: The lacunarity index is a textural feature that can discriminate between differently appearing surfaces with the same fractal dimension (Plotnick et al. 1993). It is calculated by counting the number of detected pixels within an $n \times n$ moving window (we use here $n=3$). For the resulting moving-widow filtered image the coefficient of variation is calculated following Equation 4, only for non-zero values of the detected pixels. This figure gives the lacunarity index and is a measure of the variation in lumpiness of the detected pixels. In other words the feature measures whether the detected pixels form a regular pattern (low value) or an irregular pattern (high value). Obviously, this feature only gives significant information when enough pixels are detected and the resolution is high enough.

HHHV: This polarimetric measure is defined as the ratio of total power from the detected pixels in the HV image and the HH image. Note that the pixels are detected on using the HH image. A similar quantity using the HH and VV image is less useful since the HH and VV power are usually strongly correlated.

ODD and *EVEN:* These polarimetric measures refer to odd and even bounce scattering, which are defined by

$$Odd = \frac{\sigma_{hh} + \sigma_{vv} + 2\operatorname{Re}(\rho)}{2},$$ (5)

$$Even = \frac{\sigma_{hh} + \sigma_{vv} - 2\operatorname{Re}(\rho)}{2} + 2\sigma_{hv},$$ (6)

where σ are backscattering coefficients for the various polarisations and ρ the correlation coefficient of the HH and VV polarisation. The feature percent odd is defined as the percentage of detected pixels for which odd bounce scattering dominates. A pixel is said to be dominated by odd bounce scattering when the odd bounce scattering is at least twice as large as the even bounce scattering. The feature percent even is similar, but now with the even bounce scattering dominating

3.2. Results

Using the method described in the previous section we have produced for the 10 cm and 30 cm ARL-ISAR data a database of 9x794 features for the 4 targets. For the non-polarimetric MSTAR data only 6 features (radiometric and geometric) could be extracted. In Figure 4 we show the *AREA* feature as a function of aspect angle for the 10 cm ARL-ISAR data.
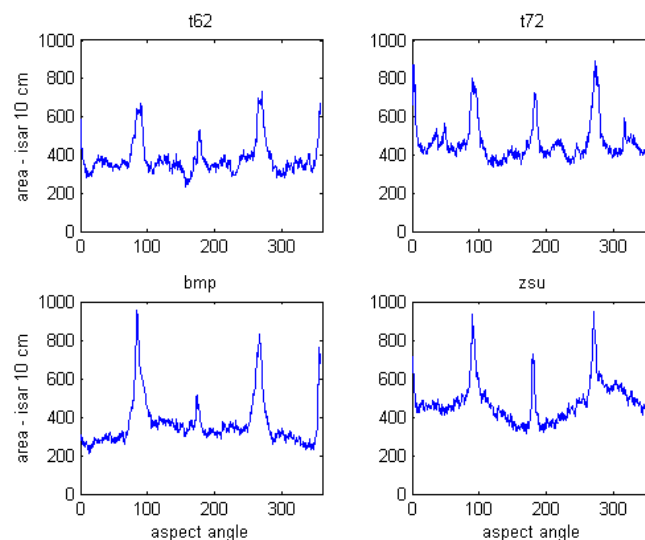
Figure 4. *AREA* feature as function of aspect angle for the 10cm ARL-ISAR data and the four targets.

4. ANALYSIS

4.1 Individual features

The individual features can be analysed from two perspectives: their invariant character with respect to the aspect angle and their capabilities to discriminate between targets. It is clear from Figure 4 that the individual features can vary significantly near aspect angles of 0°, 90°, 180°, and 270°. These aspect angles coincide with observing the targets head-on, sideways or from behind. Especially, the *AREA, MEAN, CVAR* and *HH/HV* feature show large peaks at these aspect angles. Features like the *LAC* and *WFR* show a more constant behavior as a function of aspect. The *NN* feature shows an intermediate behavior. At 0°, 90°, 180°, and 270° aspect angles *ODD* is increased, while *EVEN* is decreased, indicating that the scattering at these angles is mainly due to flat plate scattering.

The capability to discriminate the targets irrespective of the aspect angle is generally low. Either there is large variation, or the more stable features are not very distinctive. Only the area feature could discriminate between some of the targets for aspect angles other than of 0°, 90°, 180°, and 270°.

From these results, we conclude that the features vary rather dynamically as a function of aspect angle. This means that one individual feature is never capable of discriminating a target from the other targets irrespective of the aspect angle. In order to study how well we can discriminate the four targets from each other we compose feature vectors with the features extracted in the previous chapter as the constituting elements.

4.2 Feature vectors

We introduce several categories of feature vectors to see which and how many features are needed for satisfactory target discrimination. The following 5 categories of feature vectors are used

$$
\begin{aligned}
&radiometric\text{:} &&= \ [MEAN, CVAR, WFR]^T \\
&geometric\text{:} &&= \ [AREA, NN, LAC]^T \\
&polarimetric\text{:} &&= \ [HHHV, EVEN, ODD]^T \\
&generic\text{:} &&= \ [MEAN, CVAR, WFR, AREA, NN, LAC]^T \\
&generic\_pol\text{:} &&= \ [MEAN, CVAR, WFR, AREA, NN, LAC, HHHV, EVEN, ODD]^T.
\end{aligned}
$$

The feature vector containing the geometric and radiometric features is called *generic* since it can always extracted from SAR data, regardless whether the data are polarimetric or not. Of course these geometric and radiometric features only contain significant information when enough pixels can be found over the geometric extent of the target, implying that the resolution should be sufficiently high. The *generic_pol* feature vector obviously only applies to fully polarimetric data.

For the four targets we have constructed multi-variate target distributions where the elements of the distribution are the feature vectors at the various aspect angles. The number of elements of the distribution is 794, being the number of images calculated. The dimension of the multi-variate target distribution equals the number of elements in the feature vector used.

For each target distribution we calculated the mean feature vector and also the covariance matrix according to

$$
\mu_j = \frac{1}{N} \sum_{i=1}^{N} \vec{x}_i \ , \tag{7}
$$

$$
\Sigma = \frac{1}{N} \sum_{i=1}^{N} (\vec{x}_i - \vec{\mu}_j)(\vec{x}_i - \vec{\mu}_j)^T \ , \tag{8}
$$

where N=794, the number of aspects used and *j* indicates the T62, T72, BMP or ZSU target. Using these quantities we can now for each target and each aspect image calculate discriminant functions such as

$$
d_j(\vec{x}_i) = (\vec{x}_i - \vec{\mu}_j)^T \Sigma_j^{-1} (\vec{x}_i - \vec{\mu}_j) + \log(|\Sigma_j|) \ , \tag{9}
$$

where *i* is the aspect angle index and *j* is the target index. The discriminant function is derived from the Bayes' decision rule, which also takes into account the a priori probability. Since this probability is the same for each target, the a priori probability has been omitted here. This is called maximum likelihood discrimination (Duda and Hart, 1973). Note that the discriminant function is only working well under the assumption of normal distributions.

Using a feature vector for the 4 targets, we assign the target for which the discriminant function is a minimum. This procedure is repeated for every aspect angle. Next, we compute confusion matrices indicating percentages of correctly and erroneously classifications. Using this method we have produced results for all 5 categories of features vectors.

In Table 4 we show the confusion matrices for the *generic_pol* feature vector for the 10 cm and 30 cm resolution ARL-ISAR data. In Table 5 we give the average percentages of correction classification (PCC) for all feature vectors and the three cases (ARL-ISAR 10cm, ARL-ISAR 30 cm and MSTAR). Since the MSTAR data are not polarimetric only three categories of feature vectors has been studied for these data.

Table 4. Confusion matrix for feature vector category *generic_pol*

ARL-ISAR 10 cm					ARL-ISAR 30 cm				
	T62	T72	BMP	ZSU		T62	T72	BMP	ZSU
T62	84	6	8	2	T62	76	9	12	2
T72	13	73	8	6	T72	18	61	11	9
BMP	4	3	87	6	BMP	22	8	62	8
ZSU	0	5	5	90	ZSU	5	8	12	75
Average Pcc 83					Average Pcc 69				

Table 5. Average PCCs

	ARL-ISAR 10cm	ARL-ISAR 30cm	MSTAR
Radiometric	44	40	38
Geometric	66	51	47
Polarimetric	62	43	-
Generic	70	58	52
Generic_pol	83	69	-

If we inspect the confusion matrices for the 10 cm and 30 cm ARL-ISAR data we find that most of the confusion is between the T72 and T62 targets, which is not surprising, since both are main battle tanks. The average PCCs in Table 5 indicate that only the *geometric* and *polarimetric* feature vector give a reasonable discrimination between the targets with an average PCC of 66% and 62%, respectively. The *generic* feature vector gives an average PCC of 70%. When all three feature categories are combined a relatively high PCC of 83% is obtained. The increase for the PCC is mostly due to the *polarimetric* feature vector category.

For 30 cm resolution only a relatively high PCC of 69% is found for the *generic_pol* feature vector (all three categories used). All other feature vector give significantly lower PCCs. Apparently the *polarimetric* feature is quite important for discrimination both at 10 and 30 cm resolution. The *geometric* feature vector is also quite important for discrimination, but only when the resolution is sufficiently high (in the order of 10 cm).
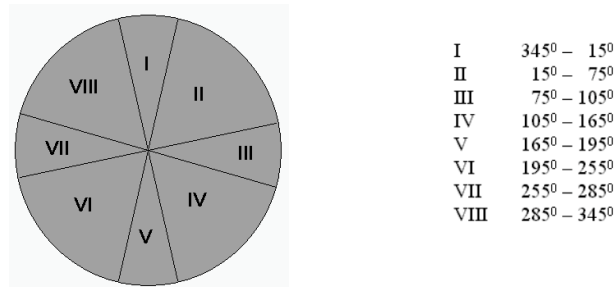
The fact that the high resolution is the reason for this characteristic of the geometrical features can also be observed in the plots for the individual features against aspect angle. The geometrical features *NN* and *AREA* are noisier and are also less discriminative between the targets at 30 cm. This is due to the fact that the number of independent scatterers on the targets is significantly decreased for 30 cm resolution compared to 10 cm resolution, implying that geometrical feature values give less discriminative information.

The average results from MSTAR data indicate that they are quite similar to 30 cm ARL-ISAR data, which can be expected due to their comparable resolutions

4.3 Analysis per aspect interval
In order to overcome the variability of the features against aspect angle and to increase the percentage of correct classification we consider here feature vectors for which the aspect angle range of 360 degrees is divided into aspect

angle intervals. In smaller aspect angle intervals feature values are more stable as a function of aspect angle. In practice when we want to apply target discrimination per aspect interval we need, of course, an efficient way to determine the aspect angle of a target. (see Section 5). We determine the discrimination between targets per aspect interval by taking the following aspect angle intervals:


I	$345^0 - 15^0$
II	$15^0 - 75^0$
III	$75^0 - 105^0$
IV	$105^0 - 165^0$
V	$165^0 - 195^0$
VI	$195^0 - 255^0$
VII	$255^0 - 285^0$
VIII	$285^0 - 345^0$

Figure 5. Overview of aspect angle intervals used.

These aspect intervals are chosen such that we can separate high backscatter (vehicle viewed head-on, sideways or from behind) and lower backscatter (vehicle viewed obliquely). Like in Section 4.2 we use feature vectors and covariance matrices and compute the discriminant functions following Equation 9, but now per aspect interval. We obtain confusion matrices for the four targets per aspect interval and in Table 6 we give the average percentages of correct classification for the different feature vectors analogous to Table 5. Figure 6 shows the behavior of the various feature vectors as function of aspect interval.

Table 6. Average PCCs

	ARL-ISAR 10cm	ARL-ISAR 30cm	MSTAR
Radiometric	47	45	57
Geometric	76	58	62
Polarimetric	59	52	-
Generic	87	67	80
Generic_pol	97	80	-
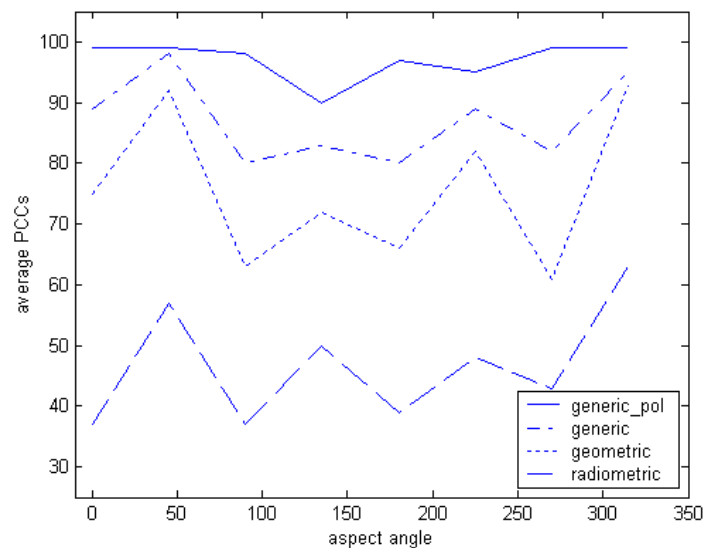
Figure 6. Average percentages of correct classification for ARL-ISAR 10 cm resolution.

The results in Table 6 show that the average PCCs are significantly higher those in Table 5. The increase is typically 10%. The generic feature vector, which can be used for non-polarimetirc data now give a PCC of almost 90% for 10 cm and 70% for 30 cm resolution. This latter result is confirmed by the results from the MSTAR data. Especially when the resolution is high enough (10 cm) and also polarimetric information is used almost complete separation is obtained between the targets. The results for the feature vectors are usually somewhat lower when the targets are viewed head-on, sideways or from behind. This is probably due to higher double bounce scatter between target and the ground, which less discriminative.

5. ASPECT ANGLE DETERMINATION

5.1 Radon transformation

For the goal of aspect determination we consider the Radon transformation of an image. The Radon transformation of an image $f(x,y)$ is defined as

$$g(\rho,\theta) = \iint f(x, y)\delta(\rho - x\cos\theta - y\sin\theta)dxdy , \qquad (10)$$

where δ denotes the Dirac delta function, θ is the rotation angle and ρ is the spatial axis parameter. Ideally a target in an image can be considered as a rectangular shape. The Radon transformation of an image containing such a shape will show a band, with peaks at the angle, for which the rectangle is seen along its long axis. Determination of the maximum in the Radon transformation image therefore gives the aspect angle. This method works well when the backscatter in the target box is homogeneous. In practice this will not be the case. We use here the image in log (dB) scaling, which suppresses variation in backscattering. However strong point scattering will also give strong peaks in the Radon transformation image and can hamper an accurate determination of the aspect angle. Also strong sidelobes due to strong scatterers will give erroneous values, typically 0 (180) or 90 (270) degrees. Figure 6 shows an example of a 10 cm ARL-ISAR image and its Radon transformation.
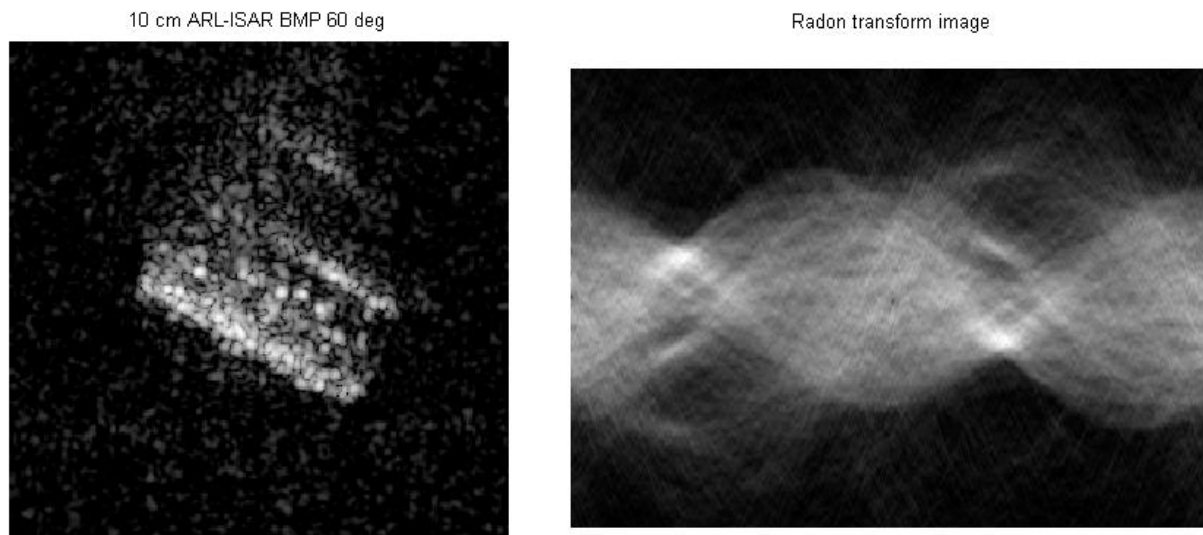

Figure 6. ARL-ISAR image and its Radon transform.

A second method to find the aspect angle is looking for the minimum of the width of the band representing the target in the Radon transform image. This method is not sensitive to interference of strong sidelobes, but is less accurate, since the outline of the band is less obvious to determine and can be influenced by the background.

Note that with these methods of aspect angle determination we cannot make distinction between head and rear of the targets. The values therefore are always between 0 and 180 degrees. In Figure 7 we have plotted the values found against the actual values for the four targets in the 10 cm and 30 cm ARL-ISAR images. We have used the aspect angle for maximum in the Radon transformation image and only in case the maximum was 0 (180) or 90 (270) degrees we used the minimum of the width of the target band in the Radon image.
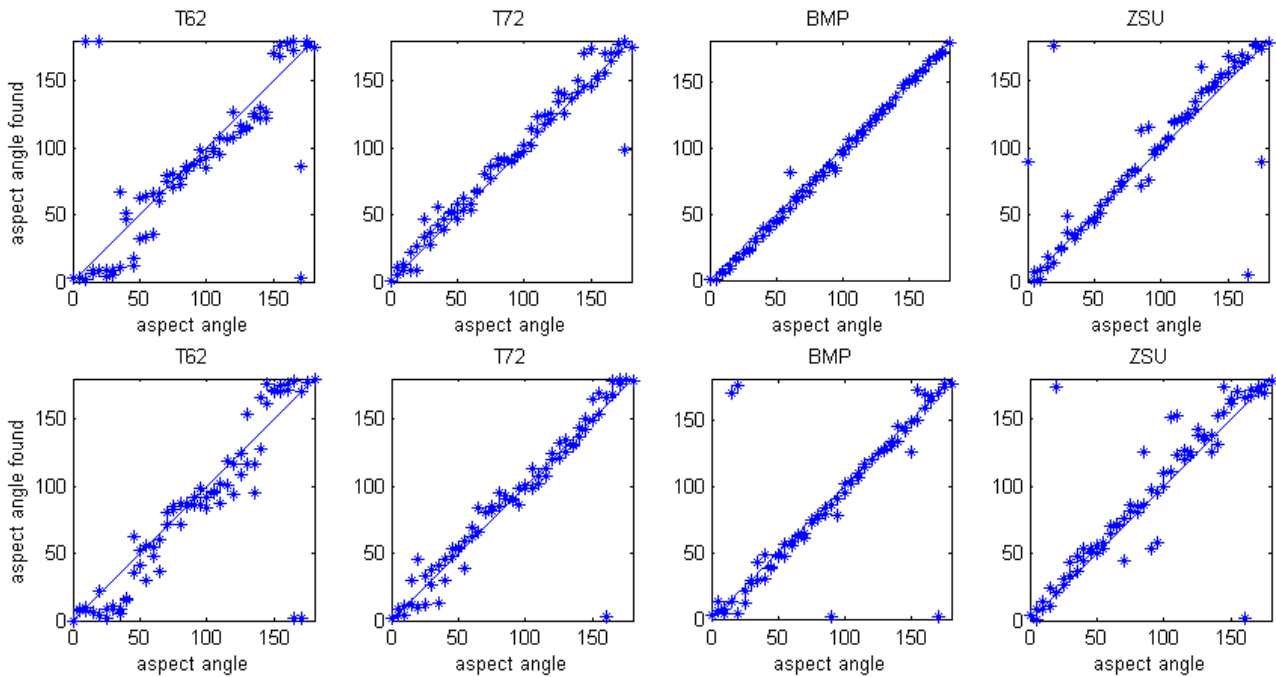

Figure 7. Aspect angles determined with Radon images versus the true aspect angle for the four targets at 10cm resoltion (top) and 30 cm resoltion (bottom).

The root mean square (RMS) error between the values found and the actual values is 13, 8, 5 and 8 degrees for the T62, T72, BMP and ZSU targets at 10 cm respectively. For the 30 cm images the RMS error is 14, 8, 6 and 9 for these targets, respectively. In the computation of the RMS error aspect angles are omitted, which are clearly erroneous. The most accurate values are found for the bmp target. This target shows rather smooth scattering at all aspect angles. The T62 target, on the other hand, does show strong point scattering at various aspect angles so that the aspect angle determination is less accurate, implying a higher RMS error and showing more scattering in Figure 7.

5.2 Region-enhanced processing
In the previous section we noted that the aspect angle determination with Radon images works best when the target box is homogeneously filled and rather constant. For this goal we applied for feature-enhanced image processing (Çetin et al. 2002) for the MSTAR data of the T72, T62, ZSU and BMP-2 targets. The processing is aimed at enhancing point features in the images or at enhancing homogeneous regions in the image. The first technique can be used to get a better separation of point scattering versus background scattering and if a finer grid is used to enhance the resolution (superresolution). The second technique can be used to better extract the target outline, and to obtain homogenous backscatterer within the target box. Figure 8 shown an example of the result after region-enhanced processing of the T62 target.
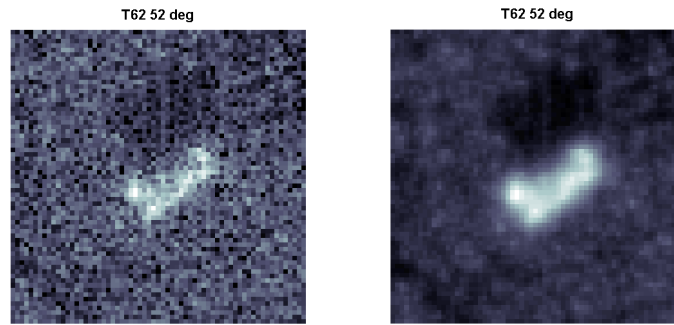
Figure 8. MSTAR data of T62 before and after region-enhanced processing.

The region-enhanced processing also suppresses the background backscatter so that a complete separation of target and backscatter pixels is possible. Using the target pixels to produce a target template, we compute the Radon transform of this template for aspect determination. In this case the outline of the band representing the target in the Radon transform can be firmly determined and the aspect angle of the minimum width of the band was used.

In Figure 9 we show the results of aspect angle determination with the Radon-transform method for the MSTAR data analogous to the one described section 5.1 and using region-enhanced processing as described above.
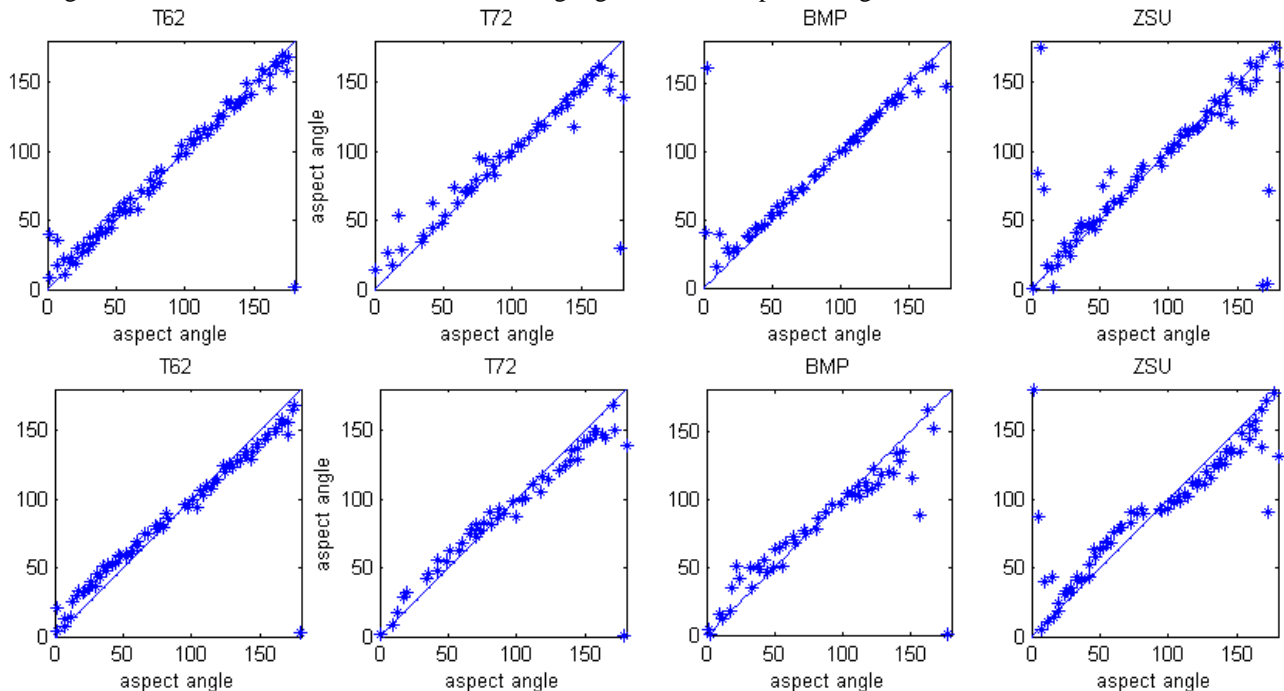
Figure 9. Aspect angles determined with Radon images versus the true aspect angle for the four targets in the MSTAR images (top) and in the region-enhanced MSTAR images (bottom).

The RMS error between the values found and the actual values is 6, 9, 6 and 8 degrees for the T62, T72, BMP and ZSU targets for the MSTAR images, respectively. Using the region-enhanced imagery the RMS error is 9, 9, 10 and 11 degrees, respectively. Like for the ARL-ISAR data the BMP target gives the more accurate values, since this target show rather smooth scattering at all aspect angles. Using the region-enhanced imagery the results are more comparable for all targets, and erroneous values due to strong scattering occur less often. However now a small systematic affect is seen, which is opposite for aspect angles smaller than 90 degrees and larger than 90 degrees, which gives relatively high RMS values. The systematic effect is probably due to the fact that the target template is not completely filled due to shadowing.

6. SUMMARY

In this study we evaluated the discrimination of targets using features from three categories: radiometric, geometric and polarimetric. Although the choice of the actual feature vectors extracted is somewhat arbitrary, we have chosen three features that give a good characterisation of each of the categories. The radiometric feature category consists of the average backscatter (*MEAN*), the variation in backscatter over the target (*CVAR*) and how much of the backscatter is found in peaks (*WFR*). The geometric feature category consists of the dimension of the target (*AREA*), a measure indicating to which degree backscatter is lumped (*NN*) and a measure indicating the regularity of the backscatter pattern of the target (*LAC*).

The polarimetric feature category consists of a measure for the backscatter from flat plates (*ODD*) and from dihedral structures on the target (*EVEN*). The third measure (*HHHV*) indicates backscatter from rough surfaces or from tilted dihedral structures.

For the study we considered three cases of data (10 cm resolution ARL-ISAR data, 30 cm resolution ARL-ISAR and MSTAR data) for four targets (T62, T72, BMP and ZSU). Using these data the features were used to discriminate the targets irrespective of the aspect angle, in order to test their robustness against variation in aspect angle. For this purpose mean values and covariance matrices were calculated for various features vectors composed of the above-mentioned individual features for the whole aspect range of 360 degrees. Using a maximum likelihood classifier targets were classified and confusion matrices were calculated as well as percentages of correct classification (PCC). When the radiometric and geometric features were used PCC values of 70%, 58% and 52% were obtained for ARL-ISAR 10 cm, ARL-ISAR 30cm and MSTAR data respectively. When also polarimetric features were used PCCs of 83% and 69 % were obtained for the polarimetric 10 cm and 30 cm ARL-ISAR data respectively

The problem for obtaining better PCC values is the variation of the features values, especially at $0°$, $90°$, $180°$, and $270°$. It could therefore be advantageous not to classify targets based on statistical information for the whole aspect range, but to do this for aspect angles intervals for which feature values are more stable. A division into intervals could be head-on, sideways, from behind and in-between.

We found that discriminating targets using aspect intervals give significantly higher PCCs up to 97% when radiometric, geometric and polarimetric features are used for the 10 cm polarimetric ARL-ISAR data.

In practice, using aspect intervals implies of course that the aspect angle has to be determined. We found that the Radon transformation is an effective tool for determining the aspect angle within an accuracy of 5–15 degrees. Using region-enhanced processing before the Radon transformation was applied a more robust method was obtained, which is less prone to erroneous values due to strong point scattering on the target.

REFERENCES

1. A.C. van den Broek, R.J. Dekker, A.J.E. Smith, and F.P.P. de Vries, "Target detection with polarimetric C-band SAR", *Proc. Of the RTO Sensors and Electronics Technology Panel (SET) Symp., High Resolution Radar Techniques, Granada, Spain, 22-24 march 1999*, RTO-MP-40, AC/323(SET)TP/8, p. 56, 1999.
2. A.C. van den Broek, R.J. Dekker, W.L. van Rossum, A.J.E. Smith, and L.J. Ewijk, "Feature extraction for automatic target recognition in high resolution and polarimetric SAR imagery", *TNO report, FEL-00-A2366, 2001*.
3. R.J. Dekker and A.C. van den Broek, "Calibration of Polarimetric PHARUS Data", *Proc. Of the CEOS SAR Workshop, Noordwijk, The Netherlands, 3-6 February 1998*.
4. C.C. Chen and H.C. Andrews, "Multifrequency Imaging of Radar Turntable Data", *IEEE Trans. on Aerosp. Electron. Syst., Vol. 16, No. 1*, pp. 15-22, 1980.
5. M. Çetin, W.C. karl, and D.A. Castañon, "Analysis of the Impact of Feature-Enhanced SAR Image on ATR Performance", *Proc.of the SPIE Conference on Algorithms for SAR imagery, IX*, vol.4742, Orlando, FL, April 2002
6. D.E. Kreithen, S.D. Halversen, and G.J. Owirka, *"Discriminating Targets from Clutter", Lincoln Laboratory Journal, Vol. 6, No. 1*, pp. 25-52, 1993.
7. R.O. Duda and P.E. Hart, *Pattern Classification and Scene Analysis*, John Wiley and Sons, New York, 1973.
8. L.M. Novak and S.R. Hesse, "On the performance of order-statistics CFAR detectors", *IEEE Conference Record of the 25th Asilomar Conference on Signals, Systems and Computers, Vol.2*, pp. 835-840, 1991.